form. The dissolved fraction (f_d) and particulate-bound fraction (f_p) are presented as follows:

$$f_d = D_m/(D_m+P_m) \quad \text{(ii)}$$

$$f_p = P_m/(D_m+P_m) \quad \text{(iii)}$$

where, D_m is the dissolved metal mass per unit volume of sample (mg); P_m is the particulate-bound metal mass per unit volume of sample (mg). For $f_d > 0.5$, the metal element mass is predominately in dissolved form. For $f_d < 0.5$, the metal element mass is mainly in particulate-bound form. The dissolved fraction (f_d) for metal elements in the roadway runoff is shown in Table 3. Based on the average dissolved fraction (f_d), the f_d value of Mo, Cr, Cd and Ni was higher than 0.5 and thus this indicated that these metal elements were transported predominately in dissolved form in the roadway runoff. The f_d values of Mn, Fe, Cu, Zn and Pb were less than 0.5 and thus this indicated that these metal elements were transported predominately in particulate-bound form in the roadway runoff. Particularly, Pb, Zn and Fe for each storm event showed strong binding to particulate matter, whereas Mo for each rainfall event was mostly presented in dissolved form in the roadway runoff.

The equilibrium fraction coefficient (K_d) for dilute solutions expresses the ratio of metal element mass normalized to the dry mass of solids to the metal element concentration in solution for a given volume of runoff. A fraction coefficient can also be used to evaluate the distribution between dissolved and particulate-bound metal elements. Thus, the fraction coefficient accounts for the presence of solids in runoff. The fraction coefficient is presented as follows:

$$K_d = C_s/C \quad \text{(iv)}$$

where, K_d is the fraction coefficient between particulate-bound mass and dissolved mass (l kg^{-1}); C_s is the particulate-bound metal element mass (mg kg^{-1} of dry solids); and C is the dissolved metal element concentration (mg l^{-1}). Table 3 also shows the fraction coefficient (K_d) for metal element in the roadway runoff. For a given mass of particulates (as SS), the K_d values computed from Eq. (iv) indicated that higher K_d values were associated with lower f_d values. Sansalone and Buchberger [4] have defined an inverse relationship between the dissolved fraction (f_d) and the fraction coefficient (K_d) for a given metal element as shown by the following:

$$f_d = 1/(1+K_d m) \quad \text{(v)}$$

where, m is the solids concentration (kg l^{-1}).

Compared to the K_d values of the other events, the higher K_d values, except Cr, of the 30 March 2004 event suggested that the high flow rate may be an important factor for the decrease of f_d values and the increase of K_d values. The high flow rate of runoff was associated with short pavement residence time of metal element in the roadway runoff. The influence of the pavement residence time and pH on metal element partitioning has been observed by other studies [4, 17].

First Flush Effect in Roadway Runoff

The first flush refers to the delivery of a disproportionately large load of pollutants during the initial period of the storm water runoff. Therefore, the normalized cumulative pollutant mass and runoff volume from the urban storm runoff are necessary information to evaluate first flush phenomenon. The normalized cumulative pollutant mass and runoff volume are represented as follows:

$$M_{nor} = m(t)/M \quad \text{(vi)}$$

Table 3. Dissolved fraction (f_d) and fraction coefficient (K_d) for metal elements.

Metal	30 Mar. 04		2 Apr. 04		4 Apr. 04		7 Apr. 04		14 Apr. 04		Mean	
	f_d	K_d	f_d	K_d	f_d	K_d	f_d	K_d	f_d	K_d	f_d	K_d
Cr	0.75	7.21	0.42	18.4	0.91	1.99	0.64	18.9	0.44	17.8	0.63	12.9
Mn	0.29	54.1	0.32	27.5	0.48	22.4	0.65	17.8	0.56	10.8	0.46	26.6
Fe	0.18	97.9	0.14	83.6	0.26	59.7	0.38	54.5	0.18	63.6	0.23	71.9
Ni	0.46	26.2	0.54	11.5	0.46	24.6	0.69	14.8	0.72	5.47	0.57	16.5
Cu	0.31	47.7	0.41	19.1	0.40	31.3	0.58	23.6	0.49	14.5	0.44	27.2
Zn	0.17	110	0.25	40.3	0.17	105	0.23	109	0.33	27.5	0.23	78.5
Mo	0.95	1.19	0.96	0.57	1.00	0.07	1.00	0.01	-	-	0.98	0.46
Cd	0.53	19.6	0.52	12.4	0.59	14.6	0.75	10.8	-	-	0.60	14.3
Pb	0.11	179	0.11	106	0.17	101	0.18	155	0.11	111	0.14	130

$$V_{nor} = v(t)/V \quad \text{(vii)}$$

where, M_{nor} is the normalized cumulative pollutant mass (dimensionless); V_{nor} is the normalized cumulative runoff volume (dimensionless); $m(t)$ is the pollutant mass transported up to time t (g); and $v(t)$ is the runoff volume up to time t (l). The first flush was observed when the cumulative mass versus volume curve was above the 45° slope line, whereas dilution occurred when the cumulative mass versus volume curve was below the 45° slope line [14]. Here, the 45° slope line represented the case when the pollutant concentration remained constant throughout the storm water runoff.

The first flush effect of the various pollutants was studied for fitting the relationship between the dimensionless cumulative pollutant mass and runoff volume in the roadway runoff as shown in Figure 4. In all cases, the cumulative mass versus volume curves were above the 45° slope line. The SS, TOC and Mo clearly showed a strong first flush, but Cr and Zn showed a weak first flush in the roadway runoff. Table 4 shows the percentages of pollutant mass transported in the first 30%, 50% and 80% of the runoff volume in the roadway runoff. Barbosa and Hvitved-Jacobsen [3] reported that the first 50% of runoff volume transported 61-69% mass of the

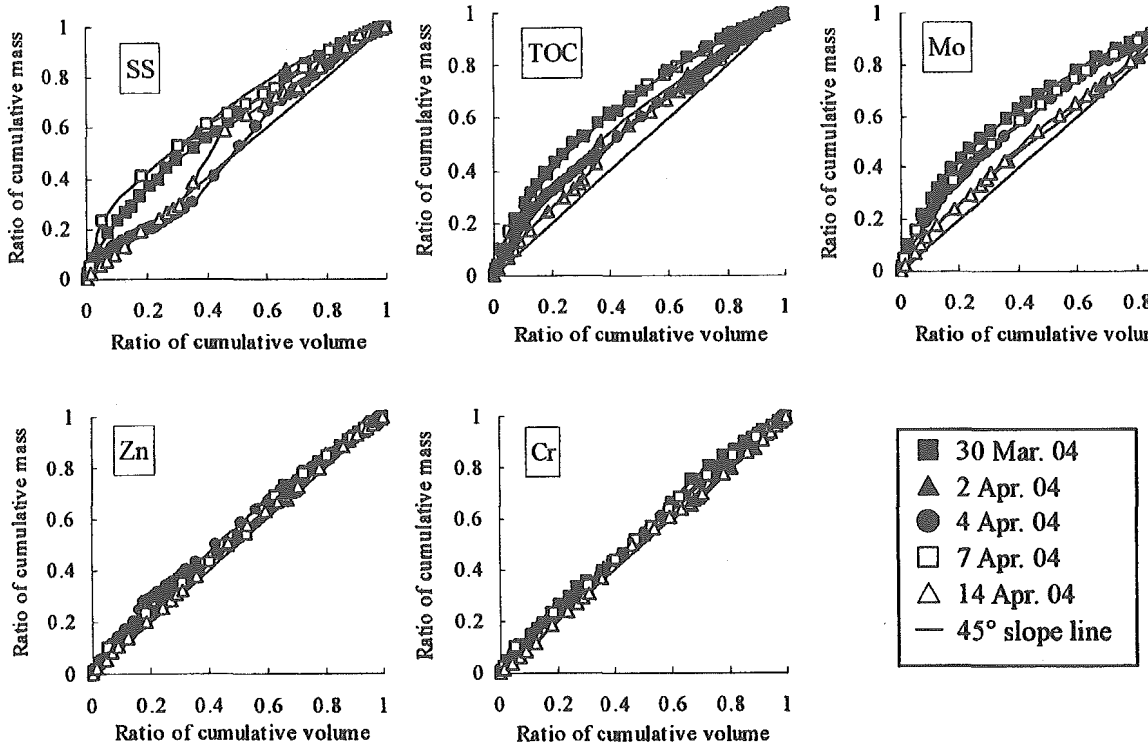

Figure 4. Examples of cumulative pollutant mass versus volume curves for storm events.

Table 4. Percentages of transported pollutants mass in the first runoff volume for five events.

Parameter	30% runoff		50% runoff		80% runoff	
	Range	Mean	Range	Mean	Range	Mean
SS	31-48	41	50-66	60	76-91	86
TOC	36-50	43	56-69	62	85-92	88
Al	30-43	37	50-62	56	79-87	83
Fe	33-48	40	52-66	59	79-90	85
Cr	29-38	34	50-56	54	81-83	82
Mn	33-42	39	53-61	59	83-89	86
Ni	35-42	39	54-61	58	82-88	85
Cu	33-44	39	53-64	59	80-91	85
Zn	33-37	35	53-58	55	82-87	83
Mo	36-51	43	56-69	62	83-91	88
Cd	32-41	38	52-60	57	80-87	84
Pb	31-44	37	52-63	57	82-86	84

TSS, Zn, Cu and Pb, and thus the Zn and Pb showed a stronger first flush effect than the TSS and Cu in the highway runoff in Portugal. Lee *et al.* [11] also reported that the SS, Fe and Pb had 30-90%, 35-85% and 40-60% range of mass transported in the first 50% of the runoff volume in the residential and industrial complex area, respectively. From Table 4, the first 50% of the runoff volume transported 62% of TOC and Mo, 60% of SS, 59% of Fe, Mn and Cu, 58% of Ni, 57% of Cd and Pb, 56% of Al, 55% of Zn, and 54% of Cr, as mean values of five storm events. The first 30% and 80% of the runoff volume also transported 34-43% and 82-88% of the mass of the pollutants, respectively. Therefore, these results showed that the first flush effect defined by 25/50 first flush [8] or by 30/80 first flush [10] was not exhibited in the roadway runoff. However, these results may be useful to correctly design treatment facilities, such as detention tanks, detention ponds, and filtration and adsorption systems, for storm water runoff.

All normalized cumulative pollutant mass versus runoff volume curves can be fitted by a power function presented as follows:

$$M_{nor} = V_{nor}^{\beta} \quad \text{(viii)}$$

where, β is the empirical coefficient. The β value is calculated by a linear regression defined as follows:

$$\ln(M_{nor}) = \beta \ln(V_{nor}) \quad \text{(ix)}$$

The first flush coefficient (β) of the pollutants for each storm event is shown in Table 5. This coefficient (β) characterized the gap between the cumulative mass versus volume curve and the 45° slope line. Thus, this gap which was used as a measure of strength of the first flush was inversely related to the first flush coefficient [10]. Lee *et al.* [11] reported that the average β values of SS and Fe were 1.80 and 1.45 for urban areas, 1.06 and 1.09 for commercial areas, 1.21 and 1.13 for industrial areas, and 0.81 and 0.89 for residential areas, respectively. Lee and Bang [9] reported that average β values of SS and Pb for industrial areas were 1.06 and 0.89, respectively, and those of SS, Pb and Fe for residential areas were 1.55, 1.06 and 1.37, respectively. Compared with these results, our data show that the average β values of SS, Pb and Fe for roadway runoff in urban area were 0.77, 0.83 and 0.77, respectively. This means that a strong first flush was exhibited in the storm water runoff from the roadway which is a small catchment area. Generally, the strength of first flush for small catchment areas is stronger than that for large catchment areas. From Table 5, the average coefficients (β) for all pollutants were all less than 1 in the roadway runoff. Based on the average coefficient (β), the relative strength of the first flush was TOC > Mo > SS and Fe > Ni and Cu > Mn > Cd > Pb> Cr > Zn in the roadway runoff.

The normalized cumulative pollutant mass (M_{nor}) and the normalized cumulative runoff volume (V_{nor}) can also be plotted as a function of normalized runoff time for each event. The maximum gap values between cumulative pollutant mass and runoff volume curves for five storm events in the roadway runoff are shown in Table 5. Based on the average maximum gap, the relative strength of the first flush was TOC (0.17) > SS (0.16) > Mn, Fe and Mo (0.15) > Ni (0.12) > Cu, Cd and Pb (0.11) > Cr and Zn (0.06) in the roadway runoff. In the case of the 30 March 2004 event, the maximum gap for all pollutants exhibited higher than the average maximum gap for five storm events, especially for TOC (0.23) and Mo (0.24) which were greater than 0.2. Therefore, these pollutants showed relatively strong first flush. This result indicated that

Table 5. Analysis results by relationship between cumulative pollutant mass and runoff volume.

Parameter	30 Mar. 04			2 Apr. 04			4 Apr. 04			7 Apr. 04			14 Apr. 04			Mean		
	a	b	c	a	b	c	a	b	c	a	b	c	a	b	c	a	b	c
SS	0.68	0.17	1.19	0.63	0.21	1.12	0.90	0.06	1.02	0.69	0.22	1.15	0.96	0.12	1.07	0.77	0.16	1.11
TOC	0.60	0.23	1.24	0.74	0.15	1.08	0.73	0.12	1.17	0.72	0.22	1.16	0.86	0.11	1.08	0.73	0.17	1.15
Al	0.84	0.10	1.08	0.71	0.17	1.09	0.95	0.11	1.06	0.78	0.10	1.07	0.97	0.03	0.99	0.85	0.10	1.06
Cr	0.87	0.09	1.07	0.76	0.04	1.01	0.92	0.04	1.05	0.88	0.05	1.04	1.03	0.04	1.00	0.89	0.05	1.03
Mn	0.76	0.18	1.14	0.72	0.16	1.07	0.83	0.13	1.15	0.80	0.17	1.11	0.94	0.09	1.05	0.81	0.15	1.10
Fe	0.75	0.16	1.13	0.62	0.20	1.11	0.89	0.09	1.05	0.69	0.20	1.14	0.91	0.10	1.05	0.77	0.15	1.10
Ni	0.78	0.18	1.15	0.73	0.10	1.05	0.87	0.08	1.07	0.74	0.14	1.09	0.89	0.09	1.07	0.80	0.12	1.09
Cu	0.75	0.14	1.15	0.68	0.11	1.06	0.87	0.04	1.05	0.73	0.19	1.14	0.95	0.08	1.06	0.80	0.11	1.09
Zn	0.90	0.06	1.05	0.86	0.04	1.03	0.86	0.10	1.12	0.91	0.06	1.03	0.94	0.05	1.03	0.90	0.06	1.05
Mo	0.59	0.24	1.24	0.75	0.06	1.03	0.73	0.17	1.23	0.74	0.18	1.14	0.87	0.08	1.07	0.74	0.15	1.14
Cd	0.78	0.15	1.13	0.75	0.13	1.07	0.81	0.13	1.15	0.82	0.09	1.04	0.94	0.06	1.02	0.82	0.11	1.08
Pb	0.81	0.13	1.11	0.68	0.15	1.08	0.85	0.10	1.10	0.82	0.09	1.03	0.98	0.07	1.03	0.83	0.11	1.07

a: first flush coefficient (β) of pollutants for storm events
b: maximum gap between cumulative pollutant mass and runoff volume
c: ratio of cumulative pollutant mass curve area to volume curve area

the first flush effect was affected by high flow rate (or rainfall intensity) in the roadway runoff. In the case of the 7 April 2004 event, the maximum gap for all pollutants, except Cr, Cd and Pb, exhibited higher than the average maximum gap for five storm events, especially for SS and TOC (0.22) and Fe (0.2) which were greater than 0.2. Therefore, these pollutants also showed relatively strong first flush. This result indicated that the first flush effect was affected by a rapid flow rate peak in the roadway runoff. Particularly, the maximum gaps of SS for the 2 April 2004 event and the 7 April 2004 event were 0.21 and 0.22, respectively. Therefore, SS was higher than 0.2 for both events that had rapid flow rate peak and showed most significant first flush in the roadway runoff. This indicated that SS was mostly infected by rapid flow rate peak in the roadway runoff more than other pollutants.

The first flush occurs when the cumulative pollutant mass curve area is in excess of the cumulative runoff volume curve area. Thus, the ratio of mass area to volume area is an index of the first flush strength. These area ratios for each storm event are also shown in Table 5. Based on the average area ratio, the relative strength of the first flush was TOC > Mo > SS > Mn and Fe > Ni and Cu > Cd > Pb > Zn > Cr > runoff volume in the roadway runoff. In the case of the 30 March 2004 event, the curve area ratios for all pollutants were greater than the average area ratios of five storm events.

CONCLUSIONS

The characteristics of pollutants from the roadway runoff and first flush effects were evaluated. The concentration of pollutants in the roadway runoff increased with increasing runoff flow in the low flow rate event, but did not significantly increase in the high flow rate event. The appearance of the peak of pollutant concentrations followed by the flow peak in the low flow rate event was more evident than that in the high flow rate event due to the fact that most of the pollutants were rapidly flushed at the beginning or early period of runoff in the high flow rate event. Additionally, the significant PSD variation in the roadway runoff occurred in high flow rate runoff.

Based on the average dissolved fraction (f_d), Mo, Cr, Cd and Ni were transported predominately in dissolved form, but Mn, Fe, Cu, Zn and Pb were transported predominately in particulate-bound form in the roadway runoff. Particularly, Pb, Zn and Fe for each storm event showed strong binding to particulate matter, whereas Mo for each storm event was presented mainly in dissolved form in the roadway runoff.

The first 50% of the runoff volume transported 62% of TOC and Mo, 60% of SS, 59% of Fe, Mn and Cu, 58% of Ni, 57% of Cd and Pb, 56% of Al, 55% of Zn, and 54% of Cr as mean values of five storm events. The first 30% and 80% of the runoff volume also transported 34-43% and 82-88% mass of the pollutants, respectively.

Based on the three parameters such as the average coefficient (β), the average maximum gap and the average area ratio, the results of the relative strength of the first flush were similar in roadway runoff. This study may also provide useful information to correctly design treatment facilities, such as detention tanks and ponds, and filtration and adsorption systems for storm water runoff from roadways.

REFERENCES

1. Boxall A.B.A. and Maltby L., The characterization and toxicity of sediment contaminated with road runoff. *Water Res.*, **29**, 2043-2050 (1995).
2. Gromaire-Mertz M.C., Garnaud S., Gonzalez A. and Chebbo G., Characterization of urban runoff pollution in Paris. *Water Sci. Technol.*, **39**, 1-8 (1999).
3. Barbosa A.E. and Hvitved-Jacobsen T., Highway runoff and potential for removal of heavy metals in an infiltration pond in Portugal. *Sci. Total Environ.*, **235**, 151-159 (1999).
4. Sansalone J.J. and Buchberger S.G., Partitioning and first flush of metals in urban roadway storm water. *J. Environ. Eng.*, **123**, 134-143 (1997).
5. Barrett M.E., Irish-Jr L.B., Malina-Jr J.F. and Charbeneau R.J., Characterization of highway runoff in Austin, Texas, area. *J. Environ. Eng.*, **124**, 131-137 (1998).
6. Deletic A.B. and Maksimovic C.T., Evaluation of water quality factors in storm runoff from paved areas. *J. Environ. Eng.*, **124**, 869-879 (1998).
7. Gupta K. and Saul A.J., Specific relationships for the first flush load in combined sewer flows. *Water Res.*, **30**, 1244-1252 (1996).
8. Wanielista M.P. and Yousef Y.A., *Stormwater management*. John Wiley & Sons, New York (1993).
9. Lee J.H. and Bang K.W., Characterization of urban stormwater runoff. *Water Res.*, **34**, 1773-1782 (2000).
10. Bertrand-Krajewski J.L., Chebbo G. and Saget A., Distribution of pollutant mass vs volume in stormwater discharges and the first flush phenomenon. *Water Res.*, **32**, 2341-2356 (1998).
11. Lee J.H., Bang K.W., Ketchum L.H., Choe J.S. and Yu M.J., First flush analysis of urban storm runoff. *Sci. Total Environ.*, **293**, 163-175 (2002).

12. Deletic A., The first flush load of urban surface runoff. *Water Res.*, **32**, 2462-2470 (1998).
13. Sansalone J.J., Koran J.M., Smithson J.A. and Buchberger S.G., Physical characteristics of urban roadway solids transported during rain events. *J. Environ. Eng.*, **124**, 427-440 (1998).
14. Geiger W.F., Flushing effects in combined sewer systems. In: *Proc. of the 4th Int. Conf. on Urban Storm Drainage*, Lausanne, Switzerland, pp. 40-46 (1987).
15. Otsu City, *Otsu Statistical yearbook.* Otsu City, Otsu (2001).
16. Ball D., Hamilton R. and Harrison R., The influence of highway-related pollutants on environmental quality. In: *Highway Pollution*, Hamilton R. and Harrison R. (eds.), Elsevier Science, New York, pp. 1-47 (1991).
17. Muschack W., Pollution of street runoff by traffic and local conditions. *Sci. Total Environ.*, **93**, 419-431 (1990).

Isolation and Identification of a New AhR Ligand 3'-Hydroxybenzo[b]quinophthalone in Dyeing Wastewater

Pei-Hsin Chou[1], Saburo Matsui[1], Kentaro Misaki[2], Tomonari Matsuda[1]

[1]Graduate School of Global Environmental Studies, Kyoto University
[2]Department of Urban and Environmental Engineering, Kyoto University

Introduction

Numerous natural compounds and environmental contaminants have been reported to activate the aryl hydrocarbon receptor (AhR)[1]. Among them, natural dye indigo and its by-product indirubin were isolated from human urine and presumed to be endogenous AhR ligands[2].A principal azo-dye methyl yellow and its halogenated derivatives were also shown to be potential xenobiotic AhR ligands, although their use has been prohibited due to the carcinogenicity[3]. It can be assumed that there are also other anthropogenic dyes which may activate the AhR, and that their residues or derivatives in industrial wastewater may cause adverse effects to aquatic environments.

In this study, a method for investigating potential AhR ligands in dyeing wastewater is presented, and 3'-hydroxybenzo[b]quinophthalone, a yellow dye chemical, was isolated and identified to be a weak AhR ligand. This method includes the applications of HPLC fractionation, a yeast bioassay[4], HPLC-diode array detector (LC-DAD), and HPLC-tandem mass spectrometry (LC-MS/MS). The analytical technique is particularly facilitated by the use of LC-MS/MS because of its high sensitivity and selectivity, which has been demonstrated to characterize dyes[5] and their derivatives[6] in environmental samples successfully.

Materials and Methods

Sampling and Extraction– Dyeing wastewater was taken from an open channel in Kyoto city, Japan, in October 2004. 1500 mL of the wastewater was filtered on 0.45 μm glass fiber filters, and passed through Sep-Pak® Vac C18 cartridges (10 g, Waters). After extraction, the cartridges were washed by water, and then eluted with 60 mL of 50% methanol in water, 60 mL of 75% methanol in water, and 120 mL of 100% methanol. The three extracts collected with respect to different eluents were evaporated to dryness in a centrifugal vacuum concentrator, and then redissolved in dimethyl sulfoxide (DMSO).

Yeast Bioassay for AhR Ligand Activity– AhR ligand activity was detected by an AhR-dependent yeast bioassay using the recombinant yeast YCM3 strain as described[2-4]. The yeast strain was grown in a synthetic glucose medium lacking tryptophan at 30℃. After 14 to 18 hours, 1 μL of the test sample was mixed with 5 μL of the saturated culture and 200 μL of the synthetic galactose medium, and subsequently incubated at 30℃. Cell density was determined by reading the absorbance at 595 nm after 18 hours of incubation, and reaction was started by throughly mixing 10 μL of the cell suspension with 140 μL of Z-buffer and 50 μL of O-nitrophenyl-β-D-galactopyranoside (4 mg/ml solution made in Z-buffer). The absorbance at 405 nm was read after incubating at 37℃ for 60 minutes. The β-galactosidase activity (reported as LacZ units) was calculated by the following formula: (absorbance at 405 nm×1000) / (absorbance at 595 nm×ml of cell suspension added×minutes of reaction time).

HPLC Fractionation, Ligand Isolation, and Purification– An aliquot of extract was injected into a C18 HPLC reversed-phase column (Shim-pack FC-ODS, 150×4.6 mm, Shimadzu), and eluted in a linear gradient of 10% to 100% methanol in water within 20 minutes followed by 100% methanol held for another 20 minutes at a flow rate of 1 mL/min. Fractions were collected every minute for 36 minutes, evaporated to dryness, redissolved in DMSO and then subjected to the yeast bioassay. After the yeast bioassay was carried out, potential AhR ligands were isolated from fractions showing AhR-mediated activity and then further purified by reversed-phase columns (Wakosil-II 5C18HG, 20×50 mm, Wako; Shim-pack FC-ODS, 150×4.6 mm, Shimadzu).

Synthesis of 3'-Hydroxybenzo[b]quinophthalone – 3'-Hydroxybenzo[b]quinophthalone was synthesized according to

the method described[7]. Equimolar amount of 2,3-naphthalenedicarboxylic acid anhydride and 3-hydroxy-2-methyl-4-quinolinecarboxylic acid were dissolved in nitrobenzene, stirred and heated overnight under reflux. Nitrobenzene was removed by distillation under reduced pressure, and then the target compound was purified by silica gel column chromotagraphy (eluent: hexane/chloroform) and recrystallization from methanol. Further purification was carried out by using reversed-phase HPLC columns.

LC/ESI-MS/MS– Experiments were carried out using the Micromass Quattro Ultima Pt mass spectrometer (Waters) equipped with a Shim-pack FC-ODS column eluted in an isocratic mode with 100% methanol at a flow rate of 0.5 mL/min. Nitrogen was used as the sheath gas; desolvation gas flow rate was set at 700 L/hr and desolvation gas temperature was 380℃. The ion source temperature was 130℃. The capillary voltage was set at 3.5 kV, and the cone voltage was 35 V. The collision energy was 30 eV for acquiring the MS/MS spectrum of synthesized 3'-hydroxybenzo [b]quinophthalone. Data acquisition was performed in the positive ion mode over thte range of m/z 50-350.

Results and Discussion

Detection of AhR Ligand activity– Compounds extracted by Sep-Pak cartridges were roughly separated into three extracts according to their polarity by using different eluents. Each extract was subjected to the yeast bioassay, and only the most hydrophobic extract (eluent: 100% methanol) elicited AhR ligand activity. 10 μL of the extract was injected into a Shim-pack FC-ODS column. Figure 1 shows the HPLC chromatogram at wavelength 456 nm and the AhR ligand activity of corresponding HPLC fractions (final concentration factor: about 5-fold of the relevant environmental concentration). The fractions collected in the 24th and 34th minutes elicited higher AhR ligand activity. According to the HPLC chromatogram, there was one major peak in the 34th fraction, which was named Yellow 1 due to its color, and its UV spectrum is shown in Figure 2. The rest of the extract was fractionated by the Wakosil-II 5C18HG column to isolate this compound, and further purification was carried out by using the Shim-pack FC-ODS column.

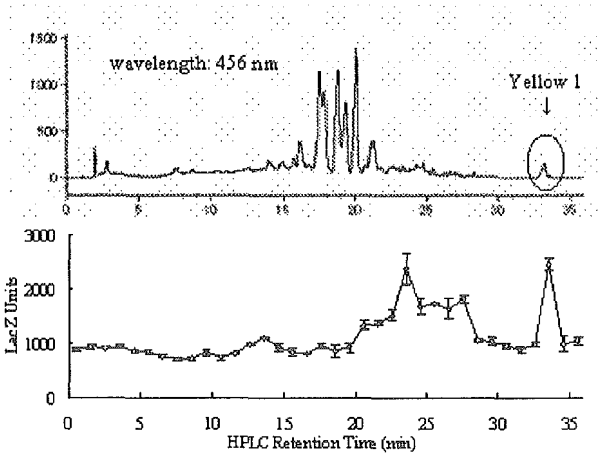

Fig 1. HPLC chromatogram and AhR ligand activity of HPLC fractions

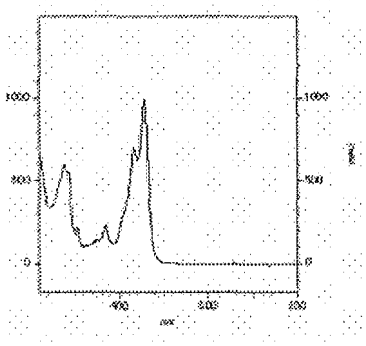

Fig 2. UV spectrum of yellow 1

Identification of Yellow 1 – Purified Yellow 1 was subjected to LC/MS/MS analysis in order to obtain more information for identification. Yellow 1 exhibited a molecular ion peak at m/z 340 in the MS spectrum. Its mass was suggested to be 339 that corresponded to the molecular weight of a yellow dye, 3'-hydroxybenzo[b]quinophthalone (3'-HB[b]QP) found in a handbook of pigments (written in Japanese) [8]. 3'-HB[b]QP was synthesized as described[7], and the HPLC retention time, UV, MS and MS/MS spectra of synthesized 3'-HB[b]QP were consistent to those of Yellow 1 . Thus, Yellow 1 was confirmed to be 3'-hydroxybenzo[b]quinophthalone.

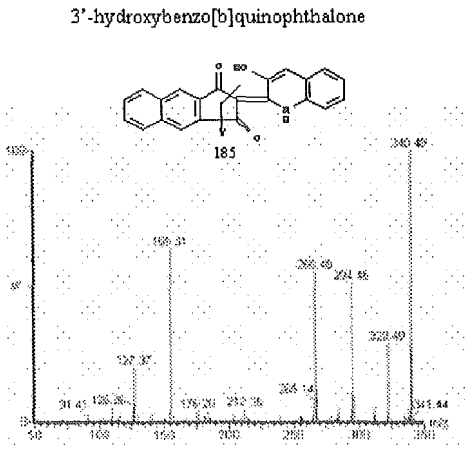

Fig 3. MS/MS spectrum of 3'-HB[b]QP

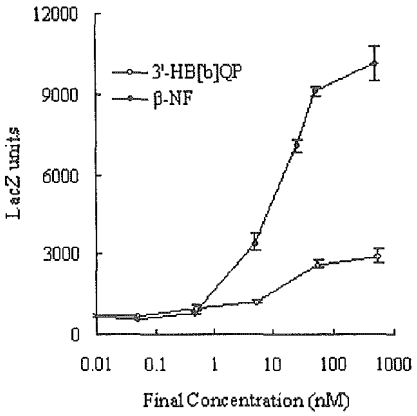

Fig 4. AhR ligand activity of 3'-HB[b]QP

Properties of 3'-Hydroxybenzo[b]quinophthalone – The MS/MS spectrum and the structure of 3'-HB[b]QP are shown in Figure 3. Figure 4 shows the dose-response curve of the AhR ligand activity of 3'-HB[b]QP comparing to an archetypal AhR ligand, β-naphthoflavone (β-NF). Although 3'-HB[b]QP only showed weak AhR ligand activity, it was able to induce signaling in the YCM3 strain at nanomolar concentrations.

3'-HB[b]QP and its brominated derivatives were studied as potential substitutes for the toxic dye cadmium yellow in Japan during 1970s. In this study, the brominated derivatives of 3'-HB[b]QP were not detected in the dyeing wastewater. However, brominated or other halogenated derivatives of 3'-HB[b]QP may also show AhR ligand activity, and sometimes the halogen-substitution might even enhance the AhR ligand activity by altering the size or planarity of the original compound[3]. Further research is necessary for monitoring the presense of these dyes in the environment as potential xenobiotic AhR ligands.

Acknowledgement

This work was supported in part by the Grant-in-Aid for Scientific research from the Ministry of Health, Labour and Welfare, and Grant-in-Aid for Scientific research from the Ministry of Education, Culture, Sports, Science and Technology, 16201012.

References

1. Denison M.S., Pandini A., Nagy S.R., Baldwin E.P. and Bonati L. (2002) *Chemico-Biological Interactions* 141: 3-24

2. Adachi J., Mori Y., Matsui S., Takigami H., Fujino J., Kitagawa H., Miller C.A. III, Kato T., Saeki K. and Matsuda T. (2001) *The Journal of Biological Chemistry* 34: 31475-31378

3. Kato T., Matsuda T., Matsui S., Mizutani T. and Saeki K. (2002) *Biological and Pharmaceutical Bulletin* 25: 466-471

4.Miller C.A.III (1999) *Toxicology and Applied Pharmacology* 160: 297-303

5. Preiss A., Sänger U., Karfich N. and Levsen K. (2000) *Analytical Chemistry* 72: 992-998

6. Moriwaki H., Harino H., Hashimoto H., Arakawa R., Ohe T. and Yoshikura T. (2003) *Journal of Chromatography A* 995: 239-243

7. Matsuoka M., Shiozaki H., Kitao T. and Konishi K. (1971) *Kogyo Kagaku Zasshi* 74: 1390-4 (in Japanese)

8. Okawara M., Ed. (1986) Shikiso Handbook, Kodansha, ISBN 4061396528 (in Japanese)

A natural aryl hydrocarbon receptor ligand, indirubin, causes the p21(waf1/cip1) up-regulation cooperated with tumor necrosis factor-alpha

Haruna Kaji[1], Yoshihiro Kida[2], Jun Adachi[3], Yoshitomo Mori[4], Yoshinori Sakata[1], Kenichi Saeki[5], Hajime Watanabe[6], Saburo Matsui[1], Tomonari Matsuda[1]

[1]Graduate School of Global Environmental Studies, Kyoto University
[2]Department of Engineering, Kyoto University
[3]Max-Planck Institute for Biochemistry,Department of Proteomics and Signaltransduction
[4]Japanese Ministry of the Environment
[5]Faculty of Pharmaceutical Sciences, Nagoya City University
[6]Okazaki Institute for Integrative Bioscience, National Institutes for Natural Science

Introduction

Indirubin, isolated from human urine, is a natural ligand of the aryl hydrocarbon receptor (AhR) and has 50 times stronger AhR activating activity when compared to 2,3,7,8-tetrachrolodibenzo-*p*-dioxin in the yeast assay for AhR ligand activity.[1] We previously reported that cell-cycle arrest and cell differentiation occurred when human lymphoma cell line ML-1 was co-treated with indirubin and tumor necrosis factor-alpha (TNF-a) in DIOXIN2003. Further investigation showed that cell cycle arrest occurred in the G1 phase and that p53-independent up-regulation of the cyclin-dependent kinase inhibitor, $p21^{(waf1/cip1)}$, is involved with this phenomenon (unpublished data). In the p21 promoter region, many transcription factor binding sites are included, and many p53-independent p21 activation pathways exist.[2] To determine which transcription factors and which p21 activation pathways are mainly involved with this up-regulation is of importance. In this study, we first constructed a firefly luciferase vector containing p21 promoter regions of various lengths. After which, the region that mainly relates to the up-regulation of p21 was evaluated and the candidate transcriptional factor binding sites that take part in cell-cycle arrest were explored using a reporter gene assay.

Materials and Methods

Materials Indirubin was synthesized as described previously and kindly provided by Dr. Saeki (Nagoya City University, Nagoya, Japan).[3] Vectors and the Dual-Glo™ luciferase assay system were purchased from Promega (Wisconsin, USA). Oligonucleotides were purchased from SIGMA genosys (Hokkaido, Japan). Restriction enzymes, T4 polynucleotide kinase, T4 Ligase, TaKaRa Ex Taq® R-PCR Version 2.1 and DNA ligation kit ver.2.1 were purchased from TaKaRa Bio Inc. (Shiga, Japan). All other chemicals and reagents were purchased from Wako Chemical (Osaka, Japan).

Cell culture The human breast cancer cell line MCF-7 was obtained from the Cell Resource Center for Biomedical Research, Institute of Development, Aging and Cancer, Tohoku University, Japan. The cells were grown in Dulbecco's modified Eagle's medium (DMEM) supplemented with 10% fetal calf serum at 37°C in a humidified air incubator supplemented with 5% CO_2.

Cell viability assay Cells were seeded at 1×10^4 cells per well, in 96-well plates and incubated overnight. Fresh DMEM was used and contained chemicals in various concentrations. For solvent contrast, cells were treated with DMSO (0.1% v/v). Cell viabilities were determined every 24 hours using the crystal violet method. Method details were as follows: culture media was washed and cells were stained with crystal violet by incubation with a staining solution containing 0.1% crystal violet in 10% methanol for 10 min at room temperature and rinsed gently three times in distilled water. The dye was extracted with methanol and absorbance was read at 590 nm by a micro plate reader.

Plasmids The p21 promoter DNA fragment was synthesized in three separate parts (pGLwaf459; -443~+16bp, pGLwaf1587; -1571~+16bp, and pGLwaf2621; -2605~+16bp). For pGLwaf459, commercially available

oligonucleotides were phosphorylated by T4 polynucleotide kinase and bound by T4 ligase. Synthesized DNA fragments were amplified by PCR using the following oligonucleotides: 5'-CAGTGAGCTCATTAATGTCATCCTCCTGATCT-3' and 5'-TACTAGATCTAGGAACTGACTTCGG-3'. The others were generated by PCR amplification using genomic DNA extracted from ML-1 cells as the template. The oligonucleotides used as primer were as follows: 5'-CAGTGAGCTCAGGTCCTGAGGCTG TGCCGTGG-3', 5'-TCGAATTAATACATAAAAATTCAT-3' (for pGLwaf1587), 5'-CAGTGAGCTCAATTCCTCTGAAAGCTGACT-3', and 5'-GCACAGCCTCAGGACCCCACTCTA-3' (for pGLwaf2621). All DNA fragments were cloned into the Sac I andBgl IIsites of the pGL3-basic vector (which includes the firefly luciferase coding region) by using DNA ligation kit ver. 2.1. In the case of pGLwaf459, the following oligonucleotides were used as linkers; 5'-CAGTCGTACGTAGTAGC-3' and 5'- TAGCTACTACGTACGACTGAGCT-3'.

Transfection and luciferase assay Cells were seeded at 80-90% confluence in 10-cm dishes on the day before transfection. Cells were co-transfected with *Renilla* luciferase expressing vector, pRL-TK, as an internal control, using lipofectamine 2000 reagent according to the manufacturer's instructions. Six hours later, the transfection reagent was removed and cells were harvested into 12-well plates. Twenty-four hours after transfection, cells were treated with chemicals and DMSO. Following 12 hours of incubation, cells were collected and dissolved in 75 ml of DMEM without serum and phenol red, and firefly and *Renilla* luciferase activities were measured using the Dual-Glo^{TM} luciferase assay system according to manufacturer's instructions. Each assay was practiced three times.

Results and Discussion

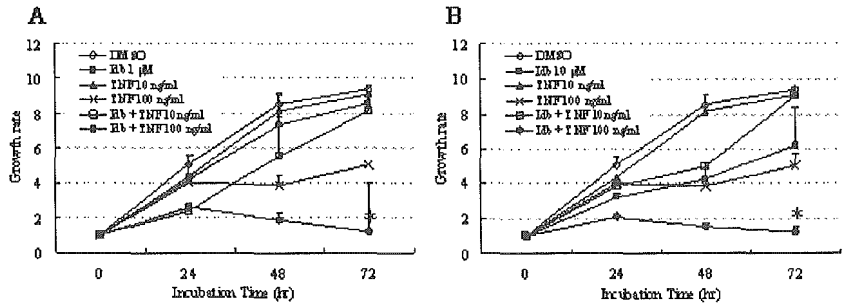

Fig. 1 MCF-7 was seeded at 1×10^4 cells per well, in 96-well plates and after overnight incubation, cells were treated with tested chemicals or DMSO (0.1% v/v). Cell viabilities were determined every 24 hours using crystal violet. When they were co-treated with indirubin (**A**: 1 μM and **B**: 10 μM) and TNF-a (100 ng/ml)? these chemicals synergistically arrested cell growth similarly.
* Significantly different from DMSO ($p < 0.05$)

Cell viability To examine whether cell growth arrest in the ML-1 cell line was also observed in the MCF-7 cell line, cell viabilities after exposure to indirubin and TNF-a at various concentrations were determined. When cells were exposed to indirubin or TNF-a only, results indicated that cell growth arrest was not observed at any concentration. However, when cells were co-treated with indirubin (≥1 mM) and TNF-a (100ng/ml), these chemicals synergistically caused arrested cell growth regardless of the concentration of indirubin as long as it was above 1 mM (Fig. 1). The effective concentration was three orders of magnitude greater than that of ML-1. Considering that indirubin is rapidly metabolized by CYP1A1 induced by itself, the potency of induction of CYP1A1 might be different between MCF-7 and ML-1.[4] Further research such as measuring the difference of the metabolic rate of indirubin and TNF-a in MCF-7 and ML-1 should be required.

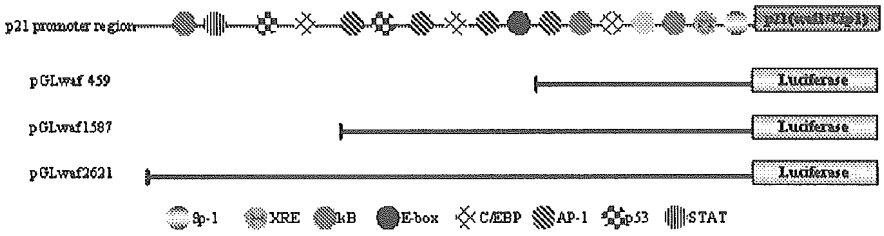

Fig. 2 The vector constructs and major transcription factor binding sites are represented. The p21 promoter region was cloned into pGL3-basic which expresses the firefly luciferase gene. Each vector contained several important binding sites for activating p21 gene.

Luciferase activity Previous research has revealed that the peak of induction of p21 mRNA was 8 hours later from the point when stimulation started (unpublished data), therefore, we decided upon an exposure time of 12 hours after considering the time for protein synthesis in this study. Firstly, changes in luciferase activities with various concentrations of indirubin were determined using pGLwaf2621. As shown in Fig. 2A, in the case of co-treatment of indirubin and TNF-a, the luciferase activities were significantly different at all concentrations ($p < 0.01$). In addition, the luciferase activity intensity was changed in a concentration-dependent manner after 12 hours of exposure. The same results were also observed in pGLwaf459 and pGLwaf1587 (data not shown). In order to obtain more clear data, the exposure concentration of indirubin was decided to be 10 mM in this study. Fig. 2B shows the pattern of luciferase induction for three vectors we investigated. In all vectors, the luciferase activity was higher when cells were exposed to both indirubin and TNF-a. However the differences in luciferase induction patterns as related to chemical exposure were not observed. Therefore, it seems that the transcription factor binding sites included in pGLwaf459 are mainly associated with this p21 induction as caused by combined exposure of indirubin and TNF-a. In the region -443~+16, many transcription factor binding sites exist, for example AP-1, kB, XRE, and Sp-1, and they play important roles in p53-independent p21 regulation. It is natural to regard that these two transcription factor binding sites, AhR, which is activated by indirubin and associates with XRE, and NF-kB which is activated by TNF-a and associates with kB, caused this p21 up-regulation. Indeed, several studies have reported the relationship between XRE and kB in genes which have both binding sites within their promoter region.[5, 6] However, with respect to p21, it was reported that one natural ligand of AhR, 3, 3'-diindolylmethane, activates the Sp-1 sites of p21 and promotes p21 protein synthesis and therefore that AhR has a relationship to Sp-1.[7, 8] Considering these facts, further research is required for revealing the mechanism of p21 up-regulation combined with the effects of indirubin and TNF-a using shorter reporter vectors other than pGLwaf459.

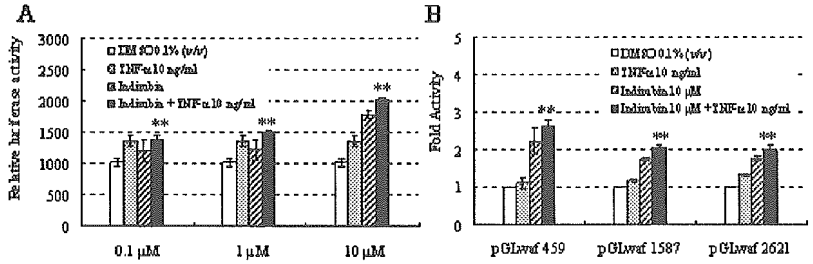

Fig. 3 The results of luciferase assay. **A**: The change in luciferase activities with various concentrations of indirubin was determined using pGLwaf2621. MCF-7 cells were co-transfected with pGLwaf2621 and pRL-TK. Twenty-four hours later, cells were treated with chemicals or DMSO (0.1% v/v). After 12 hours of incubation, the firefly and *Renilla* luciferase activity were measured. The intensity of luciferase induction changed in concentration-dependent manner. **B**: The pattern of luciferase induction related to the plasmids was determined. The method of measurement was the same as **A**. The bars show the average data of the fold activity of luciferase induction versus DMSO (0.1% v/v). The pattern of luciferase induction did not changed among the three vectors, pGLwaf459, pGLwaf1587, and pGLwaf2621. The extent of induction change was not very different among vectors. ** shows that the data were significantly different from DMSO ($p<0.01$).

In this research, we constructed a reporter vector that included that codes for the longest p21 promoter region (-2605~+16) and our experiment revealed that the specific region where ligand binding occurs is located in the region from -443 to +16 of the p21 promoter. However, the exact sequence which functions as the ligand binding site is still

unclear, therefore, further research to reveal the specific binding site is required. For example, it may be appropriate to use the luciferase assay with a shorter vector than that used in this research, or to use the electro mobility shift assay.

Acknowledgements

This work was partially supported by "Ministry of Health, Labour and Welfare" and "grant in aid for scientific research, Ministry of Education, Culture, Sports, Science and Technology".

References

1. Adachi J., Mori Y., Matsui S., Takigami H., Fujino J., Kitagawa H., Miller C A 3rd., Kato T., Saeki K. and Matsuda T. (2001) *J. Biol. Chem.* 276: 31475-31478

2. Gartel A.L. and Tyner A.L. (1999) *Exp. Cell Res.* 246: 280-289

3. Hoessel R., Leclerc S., Endicott J.A., Nobel M.E.M., Lawrie A., Tunnah P., Leost M., Damiens E., Marie D., Marko D., Niederberger E., Tang W., Eisenbrad G. and Meijer L. *Nat. Cell Biol.* 1: 60-67

4. Adachi J., Mori Y., Matsui S. and Matsuda T. (2004) *Toxicol. Sci.* 80: 161-169

5. Tian Y., Ke S., Denison M.S., Rabson A.B. and Gallo M.A. (1999) *J. Biol. Chem.* 274: 510-515

6. Kim D.W., Gazourian L., Quadri S.A., Romieu-Mourez R., Sherr D.H. and Sonenshein G.E. (2000) *Oncogene* 19: 5498-5006

7. Hong C., Kim H.A., Firestone G.L. and Bjeldanes L.F. (2002) *Carcinogenesis* 23: 1297-1305

8. Kobayashi A., Sogawa K. and Fujii-Kuriyama Y. (1996) *J. Biol. Chem.* 271: 12310-12316

Detection and identification of dyes showing AhR binding affinity in treated sewage effluents

Pei-Hsin Chou, Saburo Matsui, and Tomonari Matsuda
Department of Technology and Ecology, Graduate School of Global Environmental Studies, Kyoto University, Sakyo-Ku, Yoshida-Honmachi, Kyoto, 606-8501, Japan

Abstract A bioassay using the YCM3 recombinant yeast strain was utilized to investigate the presence of dioxin-like compounds that activate the aryl hydrocarbon receptor (AhR) in treated sewage effluents. AhR ligand activity was detected in the concentrated extracts of effluent samples collected in March, June and October 2004 from Kyoto city, Japan. HPLC fractionation was carried out using C18 reversed-phase columns, and possible AhR ligands were further isolated and purified. By using LC/MS/MS, one weak AhR ligand was identified to be rhodamine B base, a fluoran dye. In addition, two other colored ligands were postulated to be disperse anthraquinone dyes or their metabolites due to their UV spectra and HPLC retention times. The AhR binding affinities of twelve commercial dyes with different chemical structures were also studied. Among the dyes tested, hydrophobic anthraquinone dyes exhibited higher AhR ligand activity, but azo dyes or hydrophilic acid dyes showed no or very low AhR ligand activity. Rhodamine B base and disperse anthraquinone dyes were suggested to be potential xenobiotic AhR ligands. Future research regarding their contamination in aquatic environments and toxicological information is necessary.
Keywords Aryl hydrocarbon receptor; dyes; treated sewage effluents

Introduction

Dyes are made to be resistant to many physical or chemical reactions, such as light, heat, acid and so forth. Some dyes, dye metabolites, and dye plant effluents have been reported to be toxic, carcinogenic or mutagenic (Hildenbrand *et al.*, 1999; Gottlieb *et al.*, 2003; Moawad *et al.*, 2003; Schneider *et al.*, 2004; Umbuzeiro *et al.*, 2004), but conventional biological treatment processes are incapable of treating many refractory dyes satisfactorily (Hutton *et al.*, 1996). Advanced chemical treatment processes may show better efficiency in removing color or COD of dyeing wastewater. However, mutagens converted from dyes by chlorination have been detected in river water (Nukaya *et al.*, 1997; Shiozawa *et al.*, 1998), and ozonation has also been indicated to increase the toxicity in synthetic dye wastewater (Hitchcock *et al.*, 2002; Kunz *et al.*, 2002).

In Kyoto city, there are many dyeing factories and their wastewaters are treated by sewage treatment plants. Treated effluents are discharged into the Yodo River system that serves as the major drinking water source for residents lived in the nearby area. In order to provide basic information for hazard assessment and reduction, monitoring of pollutants discharged into the river system is important. In this study, the presence of dioxin-like compounds that activate aryl hydrocarbon receptor (AhR) were investigated by using an AhR-dependent yeast bioassay in combination with HPLC fractionantion and LC/MS/MS identifcation. Few colored AhR ligands were detected and isolated. One compound was identified to be rhodamine B base, a fluoran dye that showed weak AhR binding affinity, and two other colored ligands were postulated to be disperse anthraquinone dyes or their metabolites. The AhR binding affinities of twelve commercial dyes with different chemical structures were also investigated by the yeast bioassay, and hydrophobic anthraquinone dyes were suggested to be potential xenobiotic AhR ligands.

Materials and methods

Materials

Rhodamine B base was purchased from Sigma-Aldrich (USA), and other dyes were provided by Nippon Kayaku (Japan). Sep-pak C18 environmental cartridges were purchased from Waters (USA). Blue rayon were purchased from Funakoshi (Japan) or synthesized as described (Hayatsu, 1992).

Sampling and extraction

Treated effluents of one sewage treatment plant located in Kyoto city, Japan, were collected in March, June, and October 2004. 2 L of effluent samples were filtered on 0.45 μm glass fiber filters, and passed through Sep-pak C18 environmental cartridges. After extraction, each cartridge was washed with 10 mL of water and then eluted with 10 mL of methanol. The eluents were combined, evaporated to dryness, redissolved in 400 μL of dimethyl sulfoxide (DMSO), and then subjected to the yeast bioassay. 100 g of blue rayon was hung in the sampling site for about 24 hours in June and October 2004 to collect enough amount of target compounds for chemial identification analysis. The extraction method was similar to that described in Nukaya *et al.* (1997). Blue rayon extracts were fractionated by HPLC to isolate potential AhR ligands.

Yeast bioassay

AhR ligand activity was measured by a yeast bioassay using the YCM3 recombinant yeast strain, a yeast containing the human AhR and aryl hydrocarbon receptor nuclear translocator (Arnt) expression construct, with a pTXRE5-Z (LacZ) reporter plasmid responded to ligand-induced AhR complex (Miller, 1999). The bioassay was carried out as described in Adachi *et al.* (2001).

HPLC fractionation, ligand isolation and purification

50 μL of the Sep-pak cartridge extract was injected into a C18 HPLC reversed-phase column (Shim-pack FC-ODS, 150×4.6 mm, Shimadzu, Japan), and eluted in a linear gradient of 10% to 100% methanol in water within 20 minutes followed by 100% methanol held for another 20 minutes at a flow rate of 1 mL/min. Fractions were collected every minute for 30 minutes, evaporated to dryness, redissolved in 50 μL of DMSO, and then subjected to the yeast bioassay. The blue rayon extracts were fractionated by another reversed-phase column (Wakosil-II 5C18HG, 20×50 mm, Wako, Japan) with a linear gradient of 75% to 100% methanol in water within 5 minutes followed by 100% methanol held for 25 minutes at a flow rate of 2.5 mL/min. Fractions were collected every 30 seconds from 7 to13 minutes, and potential AhR ligands were further isolated by HPLC columns. All HPLC experiments were undertaken at ambient temperature.

HPLC/ESI-MS/MS

Experiments were carried out using a Micromass Quattro Ultima Pt mass spectrometer (Waters, USA) equipped with a Shim-pack FC-ODS column eluted in an isocratic mode with 100% methanol at a flow rate of 0.5 mL/min. Nitrogen was used as the sheath gas; desolvation gas flow rate was set at 700 L/hr and desolvation gas temperature was 380℃. The ion source temperature was 130℃. The capillary voltage was set at 3.5 kV, and the cone voltage was 35 V. The collision energy was 25 eV for the compounds tested. Data acquisition was performed in positive ion mode.

Results and discussion

Detection of AhR ligand activity

AhR ligand activity was detected in the concentrated extracts of treated sewage effluents. As shown in Figure 1, higher AhR ligand activity was observed in the 23rd, 24th, 25th fractions (fractions collected from 22 to 25 minutes), and the 23rd fraction elicited the highest activity. According to the HPLC chromatogram (Figure 1, absorption wavelength: 540 nm), one major peak, named as Red 1 according to its color, and several smaller peaks were observed in these fractions.

Isolation and identification of AhR ligands

The main peak Red 1 in the 23rd fraction was isolated from the blue rayon extracts, and then subjected to LC/MS/MS analysis. According to the HPLC retention time, UV, MS, and MS/MS spectra, it was identified to be rhodamine B base, a fluoran dye. Though rhodamine B base was the major peak in the 23rd fraction, it only showed weak AhR binding affinity (Figure 2).

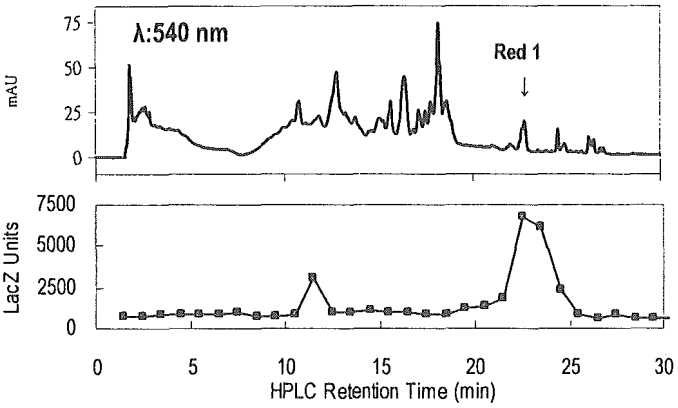

Figure 1 HPLC chromatogram of the 5000-fold Sep-pak cartridge extract and the corresponding AhR ligand activity of HPLC fractions (Oct 2004 sample)

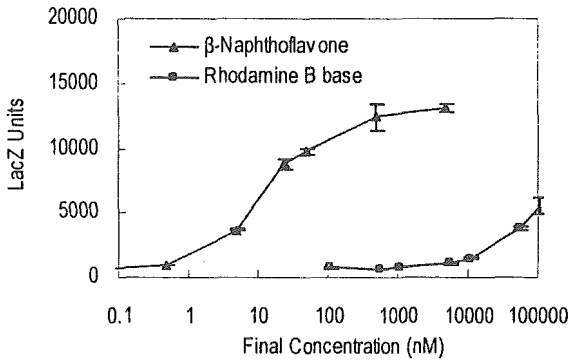

Figure 2 AhR ligand activity of rhodamine B base and an archetypal AhR ligand, β-naphthoflavone

Thus, other compounds in the same fraction were investigated by further separating the 23rd fraction into three subfractions, subsubfraction 1 (SF-1, which contained the compounds having the retention time earlier than rhodamine B base), subfraction 2 (SF-2, which contained rhodamine B base), and subfraction 3 (SF-3, which contained the compounds having the retention time later than rhodamine B base). As shown in Figure 3, SF-1 and SF-3 showed higher AhR ligand activity than SF-2. It can be suggested that the high AhR ligand activity of the 23rd fraction was mostly contributed by these unidentified compounds contained in these two subfractions.

Two other colored ligands named as Red 2 and Violet 1 were isolated from the 25th Fraction, and were suggested to be disperse anthraquinone dyes. Figure 4 shows the UV spectra and HPLC retention times of Red 2 and Violet 1 comparing to two commercial disperse anthraquinone dyes, Disperse Red 164 and Disperse Blue 56.

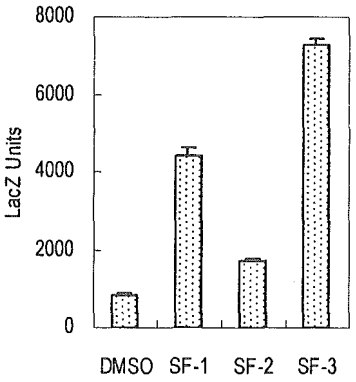

Figure 3 AhR ligand activity of the subfractions of the 23rd fraction

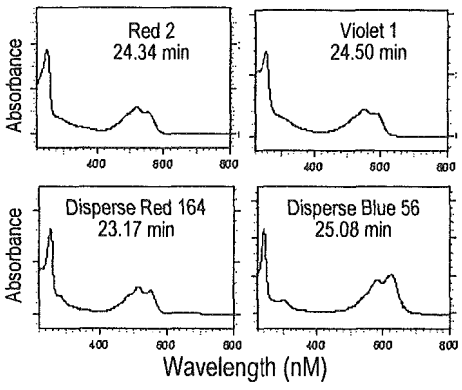

Figure 4 UV spectra and HPLC retention times of Red 2, Violet 1, Disperse Red 164, and Disperse Blue 56

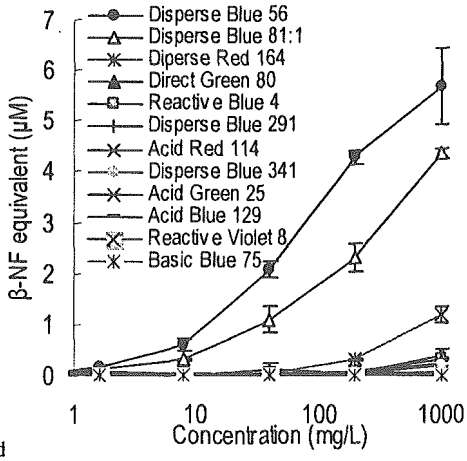

Figure 5 AhR ligand activity of commercial dyes

Disperse anthraquinone dyes as potential xenobiotic AhR ligands

Twelve commercial dyes, including three acid dyes, one basic dye, one direct dye, five disperse dyes, and two reactive dyes were also investigated for their AhR binding affinities by using the yeast bioassay. Hydrophobic anthraquinone dyes such as Disperse Blue 56 elicited higher AhR ligand activity, but no or very low activity was observed in hydrophilic acid anthraquinone dyes or azo dyes. The results corresponded to the nature of classical AhR ligands that are planar, aromatic and hydrophobic compounds.

Conclusions

In this study, AhR ligand activity was detected in treated sewage effluents, and several colored AhR ligands were isolated and suggested to be dyes. One compound was identified to be rhodamine B base, but it only showed weak AhR binding affinity and was not the most potent ligand in the 23rd fraction that elicited the highest AhR ligand activity. Two other potential AhR ligands were suggested to be disperse anthraquinone dyes or their metabolites due to their UV spectra and HPLC retention times. Disperse anthraquinone dyes such as Disperse Blue 56 also showed higher AhR binding affinity in the yeast bioassay. Rhodamine B base and disperse anthraquinone dyes are hydrophobic compounds which may be absorbed to sediments or aquatic biota after being discharged into aquatic environments. Further research concerning the contamination and ecotoxicological information of these xenobiotic AhR ligands is necessary.

Acknowledgement

This work was supported in part by the Grant-in-Aid for Scientific research from the Ministry of Health, Labour and Welfare, and Grant-in-Aid for Scientific research from the Ministry of Education, Culture, Sports, Science and Technology, 16201012.

References

Adachi J., Mori Y., Matsui S., Takigami H., Fujino J., Kitagawa H., Miller C.A. III, Kato T., Saeki K. and Matsuda T. (2001). Indirubin and Indigo are potent aryl hydrocarbon receptor ligands present in human urine. *The Journal of Biological Chemistry*, **276**, 31475-31478.

Gottlieb A., Shaw C., Smith A., Wheatley A. and Forsythe S. (2003). The toxicity of textile reactive azo dyes after hydrolysis and decolourisation, *Journal of Biotechnology*, **101**, 49-56.

Hayatsu H. (1992). Cellulose bearing covalently linked copper phthalocyanine trisulphonate as an adsorbent selective for polycyclic compounds and its use in studies of environmental mutagens and carcinogens. *Journal of Chromatography*, **597**, 37-56.

Hitchcock D. R., Law S. E., Wu J. and Williams P. L. (1998) Determining toxicity trends in the ozonation of synthetic dye wastewaters using the nematode *Caenorhabditis elefans*. *Archives of Environmental Contamination and Toxicity*, **34**, 259-264.

Hildenbrand S., SchrnalF. W., Wodarz R., Kimmel R. and Dartsch P. C. (1999). Azo dyes and carcinogenic aromatic amines in cell culture. *International Archives of Occupational and Environmental Health*, **72 (Suppl 3)**, M52-M56.

Hutton D. G., Meidl J. A., and O'Brien G. J. (1996). The PACT system for wastewater treatment. In: *Environmental Chemistry of Dyes and Pigments*, A. Reife and H. S. Freeman (ed.), Wiley, New York.

Kunz A., Mansilla H., and Durán N. (2002). A degradation and toxicity study of three textile reactive dyes by ozone. *Environmental Technology*, **23**, 911-918.

Oguri A., Shiozawa T., Terao Y., Nukaya H., Yamashita J., Ohe T., Sawanishi H., Katsuhara T., Sugimura T. and Wakabayashi K. (1998). Identification of a 2-phenylbenzotriazole (PBTA)-type mutagen, PBTA-2, in water from the Nishitakase River in Kyoto. *Chemical Research and Toxicology*, **11**, 1195-1200.

Miller C. A. III (1999). A human aryl hydrocarbon receptor signaling pathway constructed in yeast displays additive responses to ligand mixtures. *Toxicology and Applied Pharmacology*, **160**, 297-303.

Moawad H., Abd El-Rahim W. and Khalafallah M. (2003). Evaluation of biotoxicity of textile dyes using two bioassays. *Journal of Basic Microbiology*, **43**, 218-229.

Nukaya H., Yamashita J., Tsuji K., Terao Y., Ohe T., Sawanishi H., Katsuhara T., Kiyokawa K., Tezuka M., Oguri A., Sugimura T. and Wakabayashi K. (1997). Isolation and chemical-structural determination of a novel aromatic amine mutagen in water from the Nishitakase River in Kyoto. *Chemical Research and Toxicology*, **10**, 1061-1066.

Shiozawa T., Muraoka K., Nukaya H., Ohe T., Sawanishi H., Oguri A., Wakabayashi K., Sugimura T. and Terao Y. (1998). Chemical synthesis of a novel aromatic amine mutagen isolated from water of the Nishitakase River in Kyoto and a possible route of its formation. *Chemical Research and Toxicology*, **11**, 375-380.

Schneider K., Hafner C., and Jäger I. (2004). Mutagenicity of textile dye products. *Journal of Applied Toxicology*, **24**, 83-91.

Umbuzeiro G. A., Roubicek D. A., Rech C. M., Sato M. I. Z. and Claxton L. D. (2004). Investigating the sources of the mutagenic activity found in a river using the Salmonella assay and different water extraction procedures. *Chemosphere*, **54**, 1589-1597.

ELSEVIER

Molecular and Cellular Endocrinology 231 (2005) 75–85

MCE
Molecular and Cellular Endocrinology

www.elsevier.com/locate/mce

Steroid and xenobiotic receptor (SXR), cytochrome P450 3A4 and multidrug resistance gene 1 in human adult and fetal tissues

Yasuhiro Miki[a,*], Takashi Suzuki[a], Chika Tazawa[a], Bruce Blumberg[b], Hironobu Sasano[a]

[a] *Department of Pathology, Tohoku University Graduate School of Medicine, 2-1 Seiryo-machi, Aoba-ku, Sendai, Miyagi-ken 980-8575, Japan*
[b] *Department of Developmental and Cell Biology, University of California, Irvine, CA 92697-2300, USA*

Received 22 January 2004; accepted 3 December 2004

Abstract

The steroid and xenobiotic receptor (SXR) has been demonstrated to play an important role in the regulation of the cytochrome P450 3A4 gene (CYP3A4) and multidrug resistance gene 1 (MDR1) by both endogenous and xenobiotic substrates. SXR and its rodent ortholog PXR exhibit marked differences in their ability to be activated by xenobiotic inducers. This suggests that results obtained by rodent models may not always accurately predict responses to the same compounds in humans. SXR expression was demonstrated in the human liver and intestine, but its systemic distribution remains unknown. Therefore in this study, we first characterized the expression of SXR and its target genes CYP3A4, and MDR1 in human adult and fetal tissues using quantitative RT-PCR, immunoblotting, and combined laser capture microscopy and RT-PCR analysis. SXR mRNA and protein are expressed in adult and fetal liver, lung, kidney, and intestine. There is a close association between the expression of SXR and its target genes in all of the tissues examined. The amounts of SXR mRNA in the liver and intestine reached maximal levels in young adults (15–38 years old) and then subsequently decreased to less than half of the maximal levels with aging. These findings demonstrated age-related differences in the body's capacity to metabolize steroids and xenobiotic compounds and suggest an important role for SXR and its target genes, CYP3A4 and MDR1 in this process.

Keywords: Steroid and xenobiotic receptor; CYP3A4; MDR1

1. Introduction

The steroid and xenobiotic receptor, SXR (Blumberg et al., 1998a) was originally isolated as a potential homolog of the *Xenopus laevis* benzoate X receptor (Blumberg et al., 1998b). This receptor is also referred to as human pregnane X receptor (hPXR; Lehmann et al., 1998) or human pregnane activated receptor (hPAR; Bertilsson et al., 1998). SXR positively regulated transcription of cytochrome P450 3A4 (CYP3A4; Bertilsson et al., 1998; Blumberg et al., 1998a; Lehmann et al., 1998) and multidrug resistance gene (MDR1; Geick et al., 2001; Willson and Kliewer, 2002), also known as ABCB1 (ATP-binding cassette B1) and has been demonstrated to be a master or dominant regulator of xenobiotic metabolism (Synold et al., 2001; Xie and Evans, 2001; Dussault and Forman, 2002; Kliewer et al., 2002). Metabolism of drugs, xenobiotic compounds, and other endogenous/exogenous substrates such as steroids generally begins with oxidation by cytochrome P450 (CYP) phase I enzymes followed by phase II reactions in which the hydroxylated metabolite is conjugated to a polar ligand. The drug efflux pump P-glycoprotein (P-gp), encoded by MDR1 and located on the cellular plasma membrane, is the final component in these xenobiotic detoxification cascades (Michalets, 1998). The most significant cytochrome P450 for drug and xenobiotic metabolism is CYP3A, which constitutes 30 and 70% of the whole CYPs in human livers and intestines, respectively (de Wildt et al., 1999). The CYP3A subfamily consists of at least three isoforms, CYP3A4, CYP3A5 and CYP3A7 (Nelson et al., 1996). Recently, a novel isoform, CYP3A43 has been characterized (Domanski et al., 2001; Gellner et al., 2001; Westlind et al., 2001), but its functions including regulation by SXR still remains largely unknown.

* Corresponding author. Tel.: +81 22 717 8050; fax: +81 22 717 8051.
E-mail address: miki@patholo2.med.tohoku.ac.jp (Y. Miki).

0303-7207/$ – see front matter © 2004 Elsevier Ireland Ltd. All rights reserved.
doi:10.1016/j.mce.2004.12.005

Expression of CYP3A4 and CYP3A7 is induced by substrates for these enzymes largely via activation of SXR.

SXR has been demonstrated to be closely associated with the expression of CYP3A4 and MDR1 in human tissues (Bertilsson et al., 1998; Blumberg et al., 1998a; Lehmann et al., 1998; Geick et al., 2001). In addition, it is well known that the capacity for metabolism and excretion of drugs decreases with advancing age and the expression of CYP3A in human liver has been shown to vary with development (Greenblatt et al., 1982; Osterheld, 1998) but its details still remain unknown. Therefore, we hypothesized that the decreased capacity for drug and xenobiotic metabolism was related to changes in SXR expression of human tissues.

SXR was reported to be present in adult human liver, small intestine, and large intestine (Bertilsson et al., 1998; Blumberg et al., 1998a; Lehmann et al., 1998), but its cellular localization and expression in other tissues has also remained largely unknown. CYP3A and MRD1 expression has been detected in adult and fetal lung, kidney, and other human tissues (Thiebaut et al., 1987; Cordon-Cardo et al., 1990; van Kalken et al., 1992; Anttila et al., 1997; de Wildt et al., 1999) but correlation between the expressions of SXR and CYP3A or SXR and MDR1 mRNAs remain unknown. Metabolism and elimination of endogenous and exogenous substrates is very important in the fetus as well as in adults, but SXR mRNA expression in human fetal tissues is unknown. Therefore, in this study, we characterized the expression of SXR and its target genes CYP3A4, and MDR1 in human adult and fetal tissues obtained from autopsy or elective termination using quantitative RT-PCR, immunoblotting, and combined laser capture microscopy and RT-PCR analysis in order to further study the possible roles of SXR in human xenobiotic metabolisms.

2. Materials and methods

2.1. Tissue preparation

The age and gender of the subjects examined are summarized in Table 1a. The number of subjects examined in each experiment was summarized in Table 1b. The subjects have been divided into four age groups as follows: neonatal, 0 years old; young, 15–38 years old; middle aged, 45–65 years old; elderly, 67–85 years old. Human neonatal and adult livers, kidney, lung, small/large intestine, and other tissues (subjects No. 13, 15, 19, and 23) were obtained from autopsy at the Department of Pathology, Tohoku University Hospital within 2 h postmortem. Human fetal tissues (gestation ages, 14–21 weeks) were obtained after elective termination in normal pregnant woman at Nagaike Maternal Clinic (Sendai, Japan). None of the patients received corticosteroids prior to autopsy. The committee on the ethics of Tohoku University School of Medicine approved this research protocol, and informed consent for this study was obtained from pregnant women before elective termination.

2.2. Polymerase chain reaction (PCR)

2.2.1. Reverse transcription (RT)

Total RNA was extracted by homogenizing frozen tissue samples in TRIzol reagent (InVitrogen Life Technologies, Inc., Gaithersburg, ND). In order to rule out possible genomic DNA contamination, the RT step was performed in the absence of SUPERSCRIPT™ II Reverse Transcriptase (InVitrogen Life Technologies, Inc.) followed by PCR. The RT-PCR products were electrophoresed and no bands were detected in these control samples (data not shown). The re-

Table 1a
Summary of the subjects examined

No.	Age[a]	Sex	Mean[a] age	Group	No.	Age[a]	Sex	Mean[a] age	Group
1	14	M			21	44	F		
2	15	M			22	49	M		
3	18	M			23	51	M		
4	18	M	18.1	Fetus ($n=8$)	24	59	M	57.0	Middle ($n=8$)
5	19	M			25	60	M		
6	20	M			26	63	F		
7	20	F			27	65	M		
8	20	F			28	65	F		
9	0	M			29	67	F		
10	0	M	0	Neonatal[b] ($n=4$)	30	69	F		
11	0	F			31	72	F		
12	0	M			32	74	M		
13	15	F			33	75	M	75.9	Elderly ($n=8$)
14	17	M			34	81	F		
15	24	M			35	83	M		
16	28	M	28.9	Young ($n=8$)	36	86	F		
17	34	F							
18	37	M							
19	38	F							
20	38	F							

[a] Fetus, weeks; neonatal-elderly, years. M, male; F, female.
[b] No. 9, 1 day after birth; No. 10, 8 days after birth; No. 11, 14 days after birth; 12, 24 days after birth.

Table 1b
Summary of the subjects examined—the specimens number used in each experiments

Group	PCR		Immunoblotting					LCM[a]	
	Liver, kidney, lung	Intestine (small and large)	Liver	Kidney	Lung	Intestine		Kidney	Small intestine
						Small	Large		
Fetus	Nos. 1–8 ($n=8$)	No. 1, Nos. 5–8 ($n=5$)	No. 4 ($n=1$)	–	–	–	–	21 weeks M, F ($n=2$)	21 weeks M, F ($n=2$)
Neonatal	Nos. 9–12 ($n=4$)	Nos. 9–12 ($n=4$)	No. 9 ($n=1$)	–	–	–	–	–	–
Young	Nos. 13–20 ($n=8$)	Nos. 15, 17–19 ($n=4$)	Nos. 13, 19 ($n=2$)	No. 19 ($n=1$)	No. 19 ($n=1$)	No. 19 ($n=1$)	No. 19 ($n=1$)	17 years M; No. 19 ($n=2$)	–
Middle	Nos. 21–28 ($n=8$)	Nos. 21, 23, 25, 26 ($n=4$)	Nos. 21, 26 ($n=2$)	–	–	–	–	55 years M ($n=1$)	57 years M ($n=1$)
Elderly	Nos. 29–36 ($n=8$)	Nos. 29–36 ($n=8$)	No. 36 ($n=1$)	–	–	–	–	–	76 years M ($n=1$)

[a] The cases used LCM analysis different from the cases demonstrated Table 1 (except for No. 19) were used. No., demonstrated in Table 1a; LCM, laser capture microdissection; M, male; F, female; –, no specimens were available for study.

sulting cDNA was used as a template for polymerase chain reaction (PCR).

2.2.2. *Semi-quantitative real-time RT-PCR*

Real-time PCR was carried out using the LightCycler System (software version 3.5.3) with SYBR Green (LightCycler FastStart DNA Master SYBR Green I, Roche Diagnostics GmbH, Mannheim, Germany). PCR was set up at 4 mM $MgCl_2$, 10 pmol/l of each primer (Table 2; Blumberg et al., 1998a; Faneyte et al., 2001; Miki et al., 2002; Miyoshi et al., 2002) and 2.5 U *Taq* DNA polymerase (InVitrogen Life Technologies, Inc.). An initial denaturing step of 95 °C for 1 min was followed by 40 cycles, respectively, of 95 °C for 0 s; 15 s annealing at 68 °C (SXR), 62 °C (CYP3A4, and MDR1) or 60 °C (GAPDH); and extension for 15 s at 72 °C. In initial experiments, PCR products were purified and subjected to direct sequencing (ABI PRISM BigDye Terminator v3.0 Cycle sequencing Kit and ABI PRISM 310 Genetic Analyzer, Applied Biosystems, CA, USA) to verify amplification of the correct sequences. RNA from cultured human liver cells [HuH7, human hepatocellular carcinoma obtained from Cell Resource Center for Biomedical Research, Institute of Development, Aging and Cancer, Tohoku University (Sendai, Japan)] were used for SXR, CYP3A4, and MDR1 as a positive control. Negative control experiments included those lacking cDNA substrates to check for the presence of exogenous contaminant DNA. No amplified products were detected under these conditions. To determine the quantity of target cDNA transcripts, cDNAs of known concentration for SXR, CYP3A4, MDR1, and the house-keeping gene, glyceraldehyde-3-phosphate dehydrogenase (GAPDH) were used to generate standard curves for real-time qPCR. The mRNA level in each case was represented as a ratio of GAPDH, and was evaluated as a ratio (%) compared with that of each positive control. Conventional quantitative PCR requires the utilization of a defined cDNA in the construction of a standard curve, but employment of the LightCycler utilizing a purified PCR product cDNA of known concentration can semi-quantify PCR products (Miki et al., 2002).

2.2.3. *Microdissection/RT-PCR*

The specimens used microdissection/RT-PCR are summarized in Table 1b. Normal adult kidney tissues were obtained from two male patients who underwent surgical treatment for renal atrophy (17 years old) and renal cell carcinoma (55 years old), respectively. Normal adult small intestinal tissues were obtained from two male patients who underwent surgical treatment (57 and 76 years old). Fetal kidney and small intestine were obtained from the same two fetuses (18 weeks, male and female) after elective termination. Laser Capture Microdissection LCM was performed using a CRI-337 (Cell Robotics, Inc., Albuquerque, NM). Approximately 100 cells were laser-transferred from the glomerulus, urinary tubules, and the interstitium of adult and fetal kidney. Epithelium, tela submucosa and tunica muscularis of adult and fetal small intestine were also transferred. Total RNA was extracted from

Table 2
Primer sequences used in RT-PCR analysis

Cdna	GeneBank accession No.		Sequence	Size (bp)	Ref.
SXR[a]	NM022002	Forward	5′-TCC TAC ATT GAA TGC AAT CGG-3′	218	Blumberg et al. (1998a)
		Reverse	5′-CAT CAA TGC TCA GCA CAC CC-3′		
CYP3A4	NM017460	Forward	5′-CAG GAG GAA ATT GAT GCA GTT TT-3′	80	Miyoshi et al. (2002)
		Reverse	5′-GTC AAG ATA CTC CAT CTG TAG CAC AGT-3′		
MDR1	AF616535	Forward	5′-AAG CCA CGT CAG CTC TGG ATA-3′	73	Faneyte et al. (2001)
		Reverse	5′-CGG CCT TCT CTG GCT TTG T-3′		
GAPDH	M33197	Forward	5′-TGA ACG GGA GCT CAC TGG-3′	307	Miki et al. (2002)
		Reverse	5′-TCC ACC ACC CTG TTG CTG TA-3′		

[a] Oligonucleotide primers for SXR were designed using the previously published cDNA sequence.

laser-transferred cells according to a RNA microisolation protocol (Emmert-Buck et al., 1996; Niino et al., 2001). Total RNA from the microdissected kidney and intestine tissue was reverse transcribed and cDNA was amplified in 25 μl of a PCR mix consisting of GeneAmp, 1× PCR Gold Buffer (PerkinElmer Life Sciences, Inc.), 1.5 mM $MgCl_2$, 200 μM dNTP, and 0.125 unit of AmpliTaq Gold (PerkinElmer Life Sciences, Inc.) under the following conditions: initial denaturing at 95 °C for 10 min followed by 40 cycles of 1 min at 94 °C, 1 min at 55 °C, and 1 min at 72 °C, after which PCR products were subjected to a final extension step for 7 min at 72 °C. Primers used for PCR amplification were described above.

2.3. Immunoblotting

The specimens used immunoblotting are summarized in Table 1b. Approximately 100 mg of human tissues [liver, kidney, lung, spleen, stomach, small intestine, large intestine obtained from a 38-year-old woman (No. 19 in Table 1)] and livers [0,15, 24, 44, 63, and 86 years old (No. 9, 13, 21, 26, and 36 in Table 1). fetus; 18 wk (No. 4 in Table 1)] were homogenized in 500 μl of triple detergent buffer.

Immunoblotting was performed using 20 μg of protein. Following electrophoresis, protein was transferred on to Hybond P polyvinylidene difluoride membrane (Amersham Bio-

Table 3
Summary of semi-quantitative PCR for SXR, CYP3A, and MDR1

SXR expression[a]	Tissues	Age/sex		CYP3A4		MDR1	
		Adult (years)	Fetus (weeks)	Adult	Fetus	Adult	Fetus
Positive	Liver	54/M	18/F	620.0	9.7	18.7	0.2
	Kidney	54/M	18/F	0.0	0.7	50.0	2.3
	Small intestine	24/M	18/F	112.7	10.0	20.3	2.0
	Large intestine	24/M	18/F	9.7	13.0	5.0	2.1
	Lung	54/M	14/M	0.8	1.0	1.9	0.3
	Trachea	54/M	[b]	0.0		0.4	
	Heart	54/M	18/F	0.0	0.0	0.1	1.5
	Aorta	24/M	[b]	0.0		0.3	
	Esophagus	24/M	[b]	0.4		1.8	
	Stomach	24/M	[b]	0.6		1.5	
	Brain	54/M	21/F	0.0	0.5	0.9	1.0
	Pancreas	54/M	18/F	0.1		2.5	
	Spleen	54/M	18/F	0.0	0.9	3.3	0.1
	Urinary bladder	54/M	[b]	0.0		0.7	
Negative	Adrenal gland	54/M	21/M	0.7	0.4	1.7	1.2
	Thyroid	54/M	18/M	0.0	1.9	1.2	0.9
	Thymus	b	18/F		0.0		1.7
	Testis	24/M	18/M	0.3	0.2	2.3	3.0
	Prostate	24/M	[b]	0.6		3.4	
	Mammary gland	38/F	[b]	0.0		10.1	
	Fat	54/M	[b]	0.0		0.0	
	Skin	54/M	[b]	0.0		0.0	
	Muscle	15/F	[b]	0.0		0.7	
	Umbilical cord		19/M		0.1		1.3

Data are expressed on the basis of GAPDH mRNA level (%).
[a] SXR mRNA transcripts analyzed by real-time RT-PCR.
[b] No specimens were available for study.